

A review of the curious case of heat transport in Polymer Electrolyte Fuel Cells and the need for more characterization

Odne S. Burheim^a, Jon G. Pharoah^{b,*}

^a*Dep. Energy and Process Engineering, Faculty of Engineering Science, NTNU - Norwegian University of Science and Technology.*

^b*Mechanical and Materials Engineering, Queen's University at Kingston, Canada*

Abstract

As the polymer electrolyte membrane fuel cell matures performance keeps increasing - mainly in terms of conversion rate rather than efficiency. Increased conversion results in increased heat release. Fuel cell performance and degradation is a delicate balance of heat and work manipulated significantly by the transport and the state of water in the system. With high heat release rates and low thermal conductivities the maximum temperature can be up to 20°C warmer than the coolant. While much work has been done in understanding the conductivity of fuel cell materials, even more is needed. Particular needs for continued research include: the thermal implications of material ageing, the nature and importance of the composite interface between the micro-porous layer and the porous transport layer, the impact of liquid water on thermal conductivity, a better understanding of phase change in electrodes and the heat capacities of fuel cell materials. Finally, the heat release in a fuel cell presents a significant opportunity to better understand the system and changes in the system. Fuel cell calorimetry has only begun to be used to explore heat and work in PEMFC and should be explored in greater detail.

Keywords: PEMFC; Heat; Thermal Conductivity; review; Calorimetry; phase change

1. Introduction

The polymer electrolyte membrane fuel cell, PEMFC, offers electricity by converting hydrogen and oxygen into water. The technology has been around for decades and according to the USDOE, a complete system will provide a vehicle range of 600 km and weigh 90 kg by 2020 and 65-70 kg by 2030. Fuelling times will be 3.3 minutes by 2020 and 2.5 minutes by 2030[US]. They have a promising future, but there remains a need for research into the less considered thermal management and into what thermal signatures tell us about fuel cells.

An understanding of thermal effects in PEM fuel cells (and electrolyzers) is critical to increasing the reliability, durability and cost of commercial devices. In a hydrogen cell, the thermoneutral potential, or the total enthalpy change of the reaction expressed in units of V, is 1.48 V while the extraction of electrical work (0.6-0.8V or 115-155

*Corresponding author

Email addresses: burheim@ntnu.no (Odne S. Burheim), jon.pharoah@queensu.ca (Jon G. Pharoah)

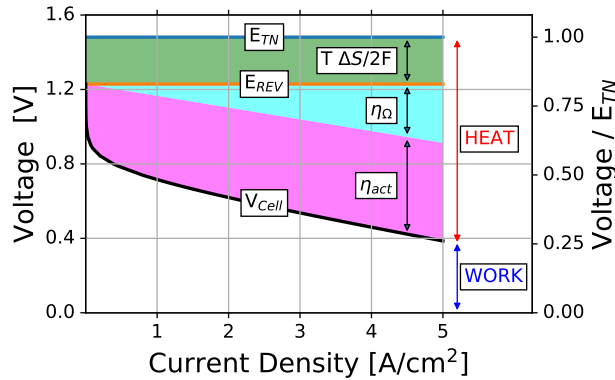


Figure 1: Heat and work of a PEM fuel cell.

10 kJ/mol_{H₂}) is necessarily accompanied by the release of heat (remaining 0.7-0.9V or 130-170 kJ/mol_{H₂}) energy due to
 11 irreversibilities and the reaction entropy change.

12 1.1. Energy - work and heat

13 The first law of thermodynamics dictates the maximum work and minimum heat output from a PEMFC. The
 14 total energy change for a given reaction (i.e. $H_2 + 1/2O_2 \rightarrow H_2O$) is given by the enthalpy change of the reaction,
 15 ΔH_r , and can be expressed in units of potential, thus defining the thermoneutral potential, $E_{TN} = -\Delta H_r/2F$. The
 16 maximum work potential is given by the Gibbs free energy change for the reaction, ΔG_r , or the reversible potential,
 17 $E_{REV} = -\Delta_r G/2F$. The minimum heat released, the reversible heat, is the negative of the reaction entropy change
 18 times the temperature, $-T_r \Delta_r S$.

19 A real fuel cell, operating away from equilibrium (i.e. drawing a current) is not thermodynamically ideal and
 20 has irreversibilities which limit the actual potential for delivered work, V_{CELL} , to less than E_{REV} with the difference
 21 released as additional heat. The two irreversibilities are the friction, or resistance, of passing protons through the
 22 membrane and catalyst layer, $\eta_{\Omega} = IR$, and the activation overpotential, η_{act} , which is mainly caused by the friction of
 23 electrons being transferred between oxygen and the catalyst. $E_{REV} - \eta_{\Omega} - \eta_{act}$. This is summarized in Figure 1 as a
 24 function of current density with the reversible heat shown in green, the heat release due to Ohmic friction in cyan, and
 25 heat due the activation overpotential shown in magenta. If the voltage is normalized by E_{TN} , as on the righthand axis
 26 of the figure, the percentage of the energy that is released as work can be read directly with the remainder released as
 27 heat.

28 1.2. More effective, efficiency remains

29 Current PEMFCs are effective hydrogen converters. That is, they convert hydrogen and oxygen into electric power
 30 and the specific conversion rate is increasingly high. A modern PEMFC uses less platinum, thinner membranes and
 31 has a smaller foot print in terms of volume and weight compared to earlier ones. These significant improvements

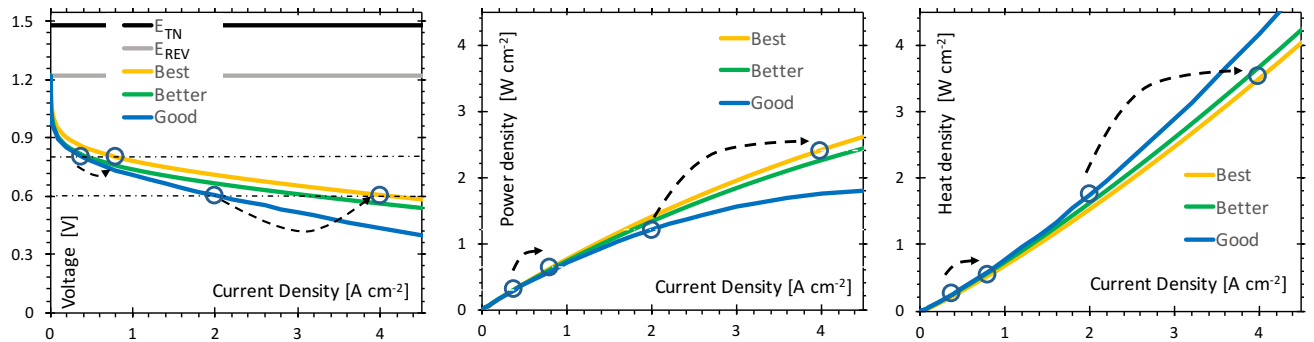


Figure 2: Polarisation curves (left), power density curves (middle) and heat generation density (right); for good, better (half membrane thickness), and best (also doubled exchange current density) fuel cell performance.

present engineering challenges as well as opportunities; as the efficiency is held constant, the specific work and heat generation are intensified. The result is stronger temperature gradients and more demanding cooling needs.

Fig. 2 presents the performance and heat rejection of a PEMFC with 'Good' kinetics [PB10], another with 'Better' performance (membrane thickness halved) and a third with 'Best' performance (additionally doubling the exchange current density). Comparing the performance of 'Good' to 'Best' at constant potentials of 0.6 and 0.8 V the efficiency (hence the losses) are by definition identical, but the current increases substantially, doubling in the case of 0.6V. As the current density increases, so does the heat density shown to the right in fig. 2 [BVMH⁺10]. Another way of saying this is that a PEMFC is improved by becoming a more effective hydrogen converter rather than a more efficient one and there is correspondingly a significant increase in heat generated.

In an engineered system, heat must be managed in order to protect component materials from excess temperatures (i.e. Nafion[ACMB01, BDWP05, RRS02]), to minimize undesired thermally driven processes (Ostwald ripening [BDG⁺06, SYG07], pinhole [LKS⁺11], local thermal stress/strain [NPCC⁺15] etc) and to maintain performance.

Fuel cells release heat primarily in the catalyst layers (CL), and the heat is ultimately rejected in the bi-polar plates after passing through the microporous layers (MPL) and the porous transport layers (PTL often referred to as GDL). These layers are particularly thin, such that the transport length is less than the order of 1 mm while the temperature difference can be in excess of 10 K resulting in temperature gradients of order 10,000 K/m. Because water is a product and the operating temperatures approach, but are below the boiling point of water, there is a strong feedback of the thermal environment to the state of water in the system and hence to performance. Furthermore, important degradation mechanisms require the presence of liquid water such that there are both direct and indirect impacts of the thermal environment on the durability of the devices.

We can learn much from the heat release and we can also make use of it, but irrespectively it must be managed.

2. Thermal Conductivity Measurements

2.1. Thermal Conductivity Determination

Experimental evidence of significant temperature differences, *i.e.* 5K, in a PEMFC was first reported by Vie and Kjelstrup [VK04]. They suggested that the thermal conductivity of membranes and PTLs was around 0.2 W K⁻¹ m⁻¹. It was already clear that thermal conductivity needed to be investigated in greater detail, with respect to materials, compression and more. Subsequently several groups investigated thermal conductivity using the heat flux method for; dry Toray and dry Nafion [KM06], procedure improvement for PTLs [RLDM08], varying water content in Nafion and in a SolviCore PTL [BVPK10], through- and in-plane thermal conductivities of dry PTLs [SDB10, SDB11, TKL11, ZLS⁺11a], the effects of PTFE content [BLP⁺11, ZLBW11] and ageing [BEF⁺13], the thermal conductivity of MPLs [BSP⁺13, BVPK10, BSK⁺16, TMD⁺14, ATKB15] and of CLs [BSH⁺14, APSB17]. Measurements of PTLs span large temperature ranges [ZLS⁺11b]. Efforts were also made in modelling, in particular for PTL with PTFE content [YANB12, SBD08], the MPL [ATKB15] and the CL [APSB17].

To summarise thermal conductivity measurements, the PTL [CKL⁺09, ZL13] is the most important component in the PEMFC because it is relatively thick (150-300 micrometers) and has different in-plane and through-plane properties [PB10]. The through-plane thermal conductivity ranges from 0.15 to 0.50 W K⁻¹ m⁻¹ depending on material, compression, and PTFE content. The presence of liquid water can increase the thermal conductivity by up to a factor of three and in the temperature range 70-85 °C even more more by the heat pipe effect [WG13], also somewhat confusingly referred to as phase change induced flow [WN06, XLCM14]. The effect of water on thermal conductivity is similar to the effects of electrolyte in supercapacitor and battery electrodes [BAAP14, BOP⁺14], where in dry electrodes the heat transfer relies solely on particle to particle contact and in wet electrodes the liquid plays an active role in bridging these contact points. The in-plane thermal conductivity can be expected to be 10-20 W K⁻¹ m⁻¹.

For MPLs, the thermal conductivity is debated among different groups and only one stand-alone MPL measurement exists. Others rely on a composite MPL/PTL, despite strong evidence showing a significant mixing region between the two. This means that there are three distinct materials: PTL, MPL, and a PTL-MPL composite. Depending on the analyses; the MPL conductivity is 0.07 W K⁻¹ m⁻¹ for stand alone measurements and 0.35 W K⁻¹ m⁻¹ or more based on composite PTL/MPLs.

The CL conductivity ranges from 0.07 to 0.21 W K⁻¹ m⁻¹, depending on type of catalyst support (non-graphitized/graphitized) and manufacturing procedure. For comparison, graphitization in battery anodes shows a threefold increase in conductivity [BOP⁺14].

Dry Nafion at room temperature has a conductivity of 0.18 W K⁻¹ m⁻¹, increasing slightly with temperature. Fully humidified, the conductivity increases to 0.26 W K⁻¹ m⁻¹, very similar to supercapacitor separators soaked in electrolyte (0.21-0.24 W K⁻¹ m⁻¹) [HPB14].

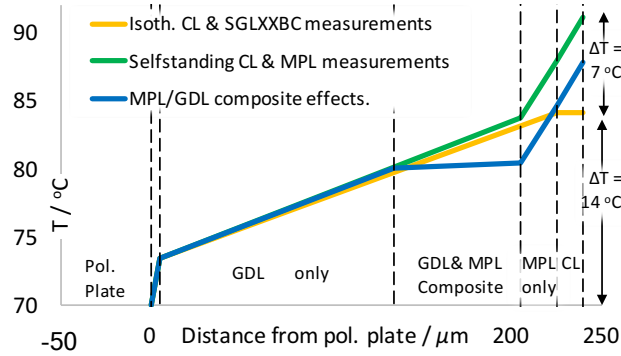


Figure 3: Temperature profiles in a series 1D model of the three cases; isothermal CL, separate MPL and CL, and MPL/PTL composite.

These values are quite low, and coupled with the significant heat releases in the CL, cause PEMFCS to be highly non-isothermal. It is important to note though that the conductivity of the PTL increases substantially in the presence of liquid water, causing a significant decrease in the temperature difference, and a decrease in evaporation rates that in turn could lead to flooding and decreased performance.

2.2. The Deviation from Isothermal, ΔT

Thus far the focus has been on conductivity, however, the resultant temperature difference is ultimately of concern. Heat is generated in the membrane/CL, and is transported in series through the CL, MPL and PTL and any contact resistances before being rejected. For the 'best' case in Fig. 2 the heat generation is 3.5 W cm^{-2} roughly equally rejected on the anode and cathode (approximately 17 kW m^{-2} each). Equation 1 gives the total resultant temperature difference (ΔT_{tot}) across a composite electrode as a function of layer conductivities (k_i), heat flux (\dot{q}) and thicknesses (δ_i).

$$\Delta T_{tot} = \dot{q} \sum_{i=1}^n \frac{\delta_i}{k_i} = \sum_{i=1}^n \Delta T_i \quad (1)$$

ΔT is of greater interest than the conductivity as the maximum temperature affects both operation (evaporation rates) and degradation rates. To illustrate the significance of a good understanding of conductivity, the temperature profiles from Eq. 1 for various cases summarized in Table 1 are presented in Fig. 3. In all cases a PTL/bi-polar plate contact resistance is included as a $5 \mu\text{m}$ air gap which is consistent with measurements [BCB⁺15, BLP⁺11].

The base case (yellow) in Fig. 3, assumes an isothermal catalyst layer, and uses measured values of SGL PTLs with and without MPLs, which were found to have very similar conductivity [BLP⁺11]. The second case (green) uses measurements of CLs [BSH⁺14] and stand-alone MPLs [BSP⁺13] having similar and low conductivities. The third case (blue) considers an inferred high conductivity for the composite region between the PTL and MPL. This region of high conductivity is reasonable based on the structure of the material, and is necessary to reconcile the low measured values of stand-alone MPLs with those of substrates with and without MPLs exhibiting the same conductivity.

Table 1: Temperature differences across PEMFC components.

| | Layer | $k /$ $\text{W K}^{-1} \text{m}^{-1}$ | $\delta /$ μm | $\Delta T /$ K |
|---|--|--|-----------------------------|----------------------------|
| 1 | PTL-bi-polar pl. [BCB ⁺ 15] | 0.025 | 5 | 3.4 |
| 2 | PTL [BLP ⁺ 11] | 0.33 | 200 | 10.3 |
| 3 | MPL [BSP ⁺ 13] | 0.08 | 20 | 4.3 |
| 4 | CL [BOP ⁺ 14] | 0.08 | 15 | 3.2 |
| 5 | PTL+MPL [BEF ⁺ 13] | 0.35* | 220 | 10.7 (14.6**) |
| 6 | PTL+PTL/MPL+MPL | 0.34*** | 220 | 11.1 |
| 7 | PTL/MPL | 4-10*** | 70 | 0.1 |

* Reported measured as composite. ** Sum of temperature drop from MPL and PTL, lines 2 and 3. *** Calculated based on what the MPL/PTL composite thermal conductivity must be for the combined MPL+PTL thermal conductivity to match the experimental value of line 5

108 Several observations are important. First, the maximum temperature is 14-21°C higher than the bi-polar plate
109 temperature, with the largest contribution due to the PTL. Second, the PTL/bi-polar plate contact contributes almost
110 3.5 °C (which would decrease significantly with condensation in this region). Third, the CL and the MPL could be
111 significant contributors, further raising the ΔT by up to 7 °C (green), but likely by 4 °C (blue). This difference warrants
112 some discussion as it clarifies apparent discrepancies in the literature and motivates additional investigation. Lines 3
113 and 4 in Table 1 represent measurements of isolated MPLs and CLs, whereas line 5 represents a single value for a
114 measured composite PTL/MPL. If these two layers were in series, then the temperature difference across the two layers
115 should be the same as that across the composite layer, but it differs by a significant 4 °C, because the interface region
116 is a composite of PTL and MPL. By choosing a dimension for this composite region (based on imaging), one can
117 estimate its conductivity which is quite high (line 7), and from this a single value for a layer made up of the substrate,
118 the composite region and the MPL (line 6) which is consistent with observation. This different interpretation results
119 in a notably different temperature in the CL, with a significant potential to impact both performance and degradation.
120 Decreased catalyst layer temperatures result in lower evaporation rates and hence in condensation rates at cooler
121 regions near the bi-polar plate where liquid water is often present [KM09, THBM08, ZW15] . This is significant,
122 because liquid water at that interface will likely eliminate the ΔT due to contact resistance, but also because liquid
123 water in the substrate can increase its conductivity by a factor of 2-3, further lowering the ΔT_{tot} and the evaporation
124 rates. This could even lead to unstable fuel cell operation,

125 2.3. Research Needs

126 It should be clear that there are significant knowledge gaps when it comes to the understanding of the thermal
127 conductivity in the MPL, the CL, and the MPL/GDL composite region. Moreover, studies comparing effects of
128 manufacturing techniques, *e.g.* air-brush, doctor blade, rolling, drying methods *etc.*, and also material impact, *e.g.*
129 material composition, carbon type, *etc.*, are missing. From Fig. 3 one can see the importance of this. In addition,
130 studies including water content variation in these layers alongside thermal conductivity values are scarce.

131 A topic mostly neglected is the effect of ageing. One study [BEF⁺13], wherein PTLs were boiled in oxygen rich
132 water for up to 1000 hours, has shown that the conductivity of dry PTLs is barely affected, however PTFE is removed
133 when the PTL ages and more water is retained such that conductivity in the presence of water increases slightly. Das
134 *et al.* [DGKW12, FSW⁺13, dBDJ08] aged PTLs (by H₂O₂ solution short boiling) and saw that this impedes water
135 removal from the surface of the GDL. This surface effect increases the water retention inside the PTL and thus agrees
136 with the previous finding, at least in the temperature range where heat-pipe [WG13] or phase-change [WN06] induced
137 flow is less important. Additional knowledge of the interplay between water, ageing and thermal conductivity of PTLs,
138 MPLs and CLs is needed.

139 3. Calorimetry - measuring heat

140 A relatively early paper on neutron imaging of water clearly demonstrated that temperature gradients have a
141 significant effect on the distribution of water in a fuel cell. Zhang *et al.* [ZKS⁺06] recorded images of a single cell
142 heated by four cartridge heaters with various combinations of the heaters on and off. In all cases the difference in
143 recorded temperatures was less than 2 °C, yet the liquid water distributions between the cases were dramatically
144 different. This observation was made theoretically as early as 2002 [DL02], and confirmed multiple times, *e.g.*
145 [FSW⁺13] and Thomas [TMD⁺13] who measured the heat flux, and water balance in a fuel cell operating with
146 different imposed temperatures on the anode and cathode and showed that the net water drag followed the temperature
147 gradient. This observation is clear when considering what has been confusingly called 'phase change driven flow'
148 [WG13, WN06, XLCM14], which describes a real flow but ascribes a completely erroneous driving force to it, but
149 it is even more interesting in considering water transport across the electrolyte which involves completely different
150 phase changes. It is clear that thermal driving forces are extremely important in fuel cells.

151 Calorimetry involves measuring the amount of heat involved in a process, and in the case of a fuel cell means
152 measuring the heat release in addition to the work obtained from the reaction. The sum of the work and the heat must
153 add up to the total enthalpy change for the reaction, which expressed in units of potential is the thermoneutral potential.
154 The first work exploring calorimetry in fuel cells was Møller-Holst *et al.* [MHKV06] which was followed up by
155 Burheim *et al.* who used calorimetric measurements to extract reaction kinetics [BVMH⁺10], but more interestingly
156 observed that below 0.6 V, the sum of the work and the heat did not equal E_{TN} . This shows definitively that the
157 reaction changes at lower potential, and they hypothesized that some of the current was generated in the production

158 of hydrogen peroxide, which has a lower reaction enthalpy. They calculated the amount of peroxide necessary to
159 achieve the measured E_{TN} , which was 15% at 0.3V. Irrespective of whether or not peroxide is produced, simultaneous
160 measurements of heat and work can definitively identify changing reaction mechanisms, be they potentially benign
161 changes in the product or the onset of degradation reactions. Simultaneous measurements of heat and work provides
162 tremendously more insight into the mechanisms occurring during power generation, and should be undertaken with
163 more regularity. Heat flux sensors in operating cells may provide additional insight and inputs to control strategies.
164 Calorimetry was also used to measure the fraction of the heat leaving the cell from the anode and cathode and from
165 this the reversible heat generation due to each electrode [BKP⁺11] was estimated. This is an important measurement
166 as it can change with reaction rate and cell design due to electro-osmotic drag [ROHS95] and saturation conditions
167 [KVA⁺13], which may help explain disagreement in the literature [Roc87, SENvS04, LF93, EBK⁺06, CW93, KIO87,
168 SS85].

169 The role of the MPL in performance improvements is well documented while the mechanism remains a matter
170 for research though liquid water is usually implicated in any such discussions. Both Atiyeh et al. [AKP⁺07] and
171 Thomas *et al.* [TMD⁺14] agree on the performance improvement and indifference of the net water balance to the
172 presence of the MPL, but by measuring heat fluxes and temperatures in the fuel cell, Thomas was able to show that
173 the additional of the MPL does result in hotter temperatures at the electrodes. This can have a tremendous impact
174 impact on performance and is a good starting point to further discuss the tight coupling between water transport,
175 heat transport and fuel cell performance. Higher temperatures result in more evaporation (and more local cooling)
176 and the strengthening the heat pipe effect which transports more reaction heat in the gas phase, potentially lowers
177 saturation levels in the PTL and results in condensation at the interface of the PTL and the bi-polar plate, which
178 serves to reduce or eliminate the thermal contact resistance there. Water is essential in most fuel cell degradation
179 mechanisms and neutron imaging has shown that changes in water distribution precede performance degradation in
180 cycling tests [FSW⁺13]. It is highly likely that the role of the MPL in improving fuel cell performance – and in
181 reducing degradation is due to this strong coupling between water transport and heat transport.

182 This suggests that more work is needed in understanding evaporation rates in electrodes. Initial work using pore
183 network models [MA10, MFIA12, FIA12] showed that pore network models were well suited to capturing evaporation
184 effects, but that evaporation rates were poorly understood. Only recently are we starting to see experiments starting to
185 address these issues [ZLE⁺16] and more of this is needed. These works suggests that pore network or hybrid models
186 may be best suited for capturing the complex interplay between water, heat and work in a PEMFC, however, their
187 transient nature will also require measurements of heat capacities which are so far non-existent.

188 4. Closing Remarks

189 PEM fuel cells are never isothermal and the amount of information that can be gleaned from isothermal models
190 is limited. A proper accounting of thermal effects should not only be incorporated in all models, but should also

191 be used as a check on the model by doing virtual calorimetry and ensuring that the work and heat do sum to the
192 overall enthalpy change [BPS14]. Fuel cells produce work, heat and water, and the balance between work is strongly
193 affected by the transport and state of water in the system, which changes the temperatures and most of the transport
194 properties through the porous materials. Water is also strongly implicated in degradation and must be managed in
195 order to increase fuel cell lifetimes. There remains significant gaps in our understanding of the interplay between
196 work, heat and water. There is also a need for additional thermal conductivity characterization with regards to the role
197 of material choices and manufacturing methods and the nature of interfaces between regions. There is also a strong
198 need to better understand the thermal implications of material ageing and the impact of liquid water on the thermal
199 properties, which also requires a much better understanding of phase change in porous fuel cell materials. Since pore
200 network type models are showing good promise for this, heat capacities of fuel cell materials are also needed. Finally,
201 this strong interplay between heat and work suggests that more fuel cell calorimetry should be explored, giving us
202 a richer understanding of both performance and changes in performance with time – heat flow sensors in fuel cell
203 systems may well provide invaluable diagnostic information.

204 References

- 205 [ACMB01] G. Alberti, M. Casciola, L. Massinelli, and B. Bauer. Polymeric proton conducting membranes for medium temperature fuel cells
206 (110-160° C). *J. Membr. Sci.*, 185:73–81, 2001.
- 207 [AKP⁺07] H.K. Atiyeh, K. Karan, B. Peppley, A. Pheonix, E. Halliop, and J.G. Pharoah. Experimental investigation of the role of a microporous
208 layer on the water transport and performance of a PEM fuel cell. *J. Power Sources*, 170:111–121, 2007.
- 209 [APSB17] M. Ahadia, A. Putz, J. Stumper, and M. Bahrami. Thermal conductivity of catalyst layer of polymer electrolyte membrane fuel cells:
210 Part I - experimental study. *J. Power Sources*, 354:215–228, 2017.
- 211 [ATKB15] M. Andisheh-Tadbir, E. Kjeang, and M. Bahrami. Thermal conductivity of microporous layers: analytical modeling and experimental
212 validation. *J. Power Sources*, 296:344–351, 2015.
- 213 * This paper presents thermal conductivity of PTL/MPL assuming the absence of a mixing region between the two
- 214 [BAAP14] Odne S. Burheim, Mesut Aslan, Jennifer S. Atchison, and Volker Presser. Thermal conductivity and temperature profiles in carbon
215 electrodes for supercapacitors. *Journal of Power Sources*, 246:160 – 166, 2014.
- 216 [BCB⁺15] Odne S Burheim, Gregory A Crymble, Robert Bock, Nabeel Hussain, Sivakumar Pasupathi, Anton du Plessis, Stephan le Roux,
217 Frode Seland, Huaneng Su, and Bruno G Pollet. Thermal conductivity in the three layered regions of micro porous layer coated
218 porous transport layers for the PEM fuel cell. *International Journal of Hydrogen Energy*, 2015.
- 219 * This paper presents the PTL/MPL composite as a three component material having an MPL region, a mixing region,
220 and a PTL region.
- 221 [BDG⁺06] Rod L Borup, John R Davey, Fernando H Garzon, David L Wood, and Michael A Inbody. PEM fuel cell electrocatalyst durability
222 measurements. *Journal of Power Sources*, 163(1):76–81, 2006.
- 223 [BDWP05] F. Bauer, S. Denele, and M. Willert-Porada. Influence of temperature and humidity on the mechanical properties of nafion 117
224 polymer electrolyte membrane. *J. Polymer Sci.: Part B*, 43:786–795, 2005.
- 225 [BEF⁺13] O. S. Burheim, G. Ellila, J. D. Fairweather, A. Labouriau, S. Kjelstrup, and J. G. Pharoah. Ageing and thermal conductivity of
226 porous transport layers used for PEM fuel cells. *Journal of Power Sources*, 221:356–365, 2013.
- 227 [BKP⁺11] O. Burheim, S. Kjelstrup, J.G. Pharoah, P.J.S. Vie, and S. Møller-Holst. Calculation of reversible electrode heats in the proton
228 exchange membrane fuel cell from calorimetric measurements. *Electrochimica Acta*, 5:935–942, 2011.

- 229 [BLP⁺11] O. Burheim, H. Lampert, J.G. Pharoah, P.J.S. Vie, and S. Kjelstrup. Through-plane thermal conductivity of PEMFC porous transport
230 layers. *Journal of Fuel Cell Science and Technology*, 8:021013–1–11, 2011.
- 231 [BOP⁺14] Odne S. Burheim, Morten A. Onsrud, Jon G. Pharoah, Fride Vullum-Bruer, and Preben J. S. Vie. Thermal conductivity, heat sources
232 and temperature profiles of li-ion secondary batteries. *ECS Transactions*, 58:145–171, 2014.
- 233 ** This paper developed the methodology of measuring conductivity on metal foils which enables the measurement of
234 thin layers such as MPLs and catalys layers. It also shows the significant difference in the conductivity of carbon upon
235 graphitization which is highly relevant to carbon supports in catalyst layers.
- 236 [BPS14] M. Bhaiya, A. Putz, and M. Secanell. Analysis of non-isothermal effects on polymer electrolyte fuel cell electrode assemblies.
237 *Electrochimica Acta*, 147:294–309, 2014.
- 238 * This paper presents a rigorous thermal model and discusses the importance of accounting for temperature gradients.
239 It also presents all the ingredients to carry out virtual calorimetry which should be carried out in all models.
- 240 [BSH⁺14] Odne S Burheim, Huaneng Su, Hans Henrik Hauge, Sivakumar Pasupathi, and Bruno G Pollet. Study of thermal conductivity of
241 PEM fuel cell catalyst layers. *International Journal of Hydrogen Energy*, 39(17):9397–9408, 2014.
- 242 * This is the first paper to present thermal conductivity measurements on isolated fuel cell catalyst layers.
- 243 [BSK⁺16] Robert Bock, Andrew Shum, Thulile Khoza, Frode Seland, Nabeel Hussain, Iryna V Zenyuk, and Odne Stokke Burheim. Experi-
244 mental study of thermal conductivity and compression measurements of the gdl-mpl interfacial composite region. *ECS Transactions*,
245 75(14):189–199, 2016.
- 246 [BSP⁺13] Odne S. Burheim, Huaneng Su, Sivakumar Pasupathi, Jon G. Pharoah, and Bruno G. Pollet. Thermal conductivity and temperature
247 profiles of the micro porous layers used for the polymer electrolyte membrane fuel cell. *International Journal of Hydrogen Energy*,
248 38:8437 – 8447, 2013.
- 249 ** This is the only paper to date to present measurements of isolated micro-porous layers and shows that pure MPLs
250 have very low conductivity.
- 251 [BVMH⁺10] O. Burheim, P.J.S. Vie, S. Møller-Holst, J.G. Pharoah, and S. Kjelstrup. A calorimetric analysis of a polymer electrolyte fuel cell
252 and the production of H₂O₂ at the cathode. *Electrochimica Acta*, 5:935–942, 2010.
- 253 [BVPK10] O. Burheim, P.J.S. Vie, J.G. Pharoah, and S. Kjelstrup. *Ex-situ* measurements of through-plane thermal conductivities in a polymer
254 electrolyte fuel cell. *Journal of Power Sources*, 195:249–256, 2010.
- 255 [CKL⁺09] L. Cindrella, A.M. Kannan, J.F. Lin, K. Saminathan, Y. Ho, C.W. Lin, and J. Wertz. Gas diffusion layer for proton exchange
256 membrane fuel cells; a review. *Journal of Power Sources*, 194(1):146 – 160, 2009.
- 257 [CW93] B.E. Conway and D.P. Wilkinson. Non-isothermal cell potentials and evaluation of entropies of ions and of activation for single
258 electrode processes in non-aqueous media. *Electrochimica Acta*, 38:997–1013, 1993.
- 259 [dBDJ08] F.A. de Bruijn, V. A. T. Dam, and G.J.M. Janssen. Review: Durability and degradation issues of PEM fuel cell components. *Fuel*
260 *Cells*, 08:1–22, 2008.
- 261 [DGKW12] Prodip K Das, Adam Grippin, Anthony Kwong, and Adam Z Weber. Liquid-water-droplet adhesion-force measurements on fresh
262 and aged fuel-cell gas-diffusion layers. *Journal of The Electrochemical Society*, 159(5):B489–B496, 2012.
- 263 [DL02] N. Djilali and D. Lu. Influence of heat transfer on gas and water transport in fuel cells. *Int. J. Therm. Sci.*, 41:29–40, 2002.
- 264 [EBK⁺06] N.R. Elezovic, B.M. Babic, N.V. Krstajic, L.M. Gajic-Krstjic, and Lj.M. Vracar. Specificity of the UPD of H to the structure of
265 highly dispersed Pt on carbon support. *Int. J. Hydrogen Energy*, 32:1991–1998, 2006.
- 266 [FIA12] D.L. Fritz III and J.S. Allen. Evaporation modelling for polymer electrolyte fuel cells. *ECS Transactions*, 50(2):113–122, 2012.
- 267 [FSW⁺13] Joseph D. Fairweather, Dusan Spornjak, Adam Z. Weber, David Harvey, Silvia Wessel, Daniel S. Hussey, David L. Jacobson,
268 Kateryna Artyushkova, Rangachary Mukundan, and Rodney L. Borup. Effects of cathode corrosion on through-plane water transport
269 in proton exchange membrane fuel cells. *Journal of The Electrochemical Society*, 160(9):F980–F993, 2013.

- 270 [HPB14] HH Hauge, V Presser, and O Burheim. In-situ and ex-situ measurements of thermal conductivity of supercapacitors. *Energy*,
271 78:373–383, 2014.
- 272 [KIO87] M. Kamata, Y. Ito, and J. Oishi. Single electrode Peltier heat of a hydrogen electrode in H₂SO₄ and NaOH solutions. *Electrochimica*
273 *Acta*, 32:1377, 1987.
- 274 [KM06] M. Khandelwal and M. M. Mench. Direct measurement of through-plane thermal conductivity and contact resistance in fuel cell
275 materials. *J. Power Sources*, 161:1106–1115, 2006.
- 276 [KM09] S. Kim and M.M. Mench. Investigation of temperature-driven water transport in polymer electrolyte fuel cell: Phase-change-induced
277 flow. *Journal of the Electrochemical Society*, 156:B353–B362, 2009.
- 278 [KVA⁺13] S. Kjelstrup, P. J. S. Vie, L. Akyalcin, P. Zefaniya, J.G. Pharoah, and O. S. Burheim. The seebeck coefficient and the peltier effect in
279 a polymer electrolyte membrane cell with two hydrogen electrodes. *Electrochimica Acta*, pages 166–175, 2013.
- 280 [LF93] M. Lampinen and M. Fomino. Analysis of free energy and entropy changes for half cell reactions. *Journal of the Electrochemical*
281 *Society*, 140:3537–3546, 1993.
- 282 [LKS⁺11] Ho Lee, Taehee Kim, Woojong Sim, Saehoon Kim, Byungki Ahn, Taewon Lim, and Kwonpil Park. Pinhole formation in PEMFC
283 membrane after electrochemical degradation and wet/dry cycling test. *Korean Journal of Chemical Engineering*, 28(2):487–491,
284 2011.
- 285 [MA10] E. Medici and J.S. Allen. The effects of morphological and wetting properties of porous transport layers on water movement in PEM
286 fuel cells. *Journal of the Electrochemical Society*, 157(10):B1505–B1514, 2010.
- 287 [MFIA12] E. Medici, D.L. Fritz III, and J.S. Allen. Diffusive and kinetic evaporation models for fuel cells. *ECS Transactions*, 50(2):113–122,
288 2012.
- 289 [MHKV06] S Møller-Holst, S. Kjelstrup, and P. Vie. In situ calorimetric measurements in a polymer electrolyte fuel cell. *The 4th International*
290 *ASME Conference on Fuel Cell Science Engineering and Technology*, pages 373–379, 2006.
- 291 [NPCC⁺15] Fredy Nandjou, Jean-Philippe Poirot-Crouvezier, Marion Chandesris, Jean-François Blachot, Céline Bonnaud, and Yann Bultel.
292 Correlation between local temperature and degradations in polymer electrolyte membrane fuel cells. *ECS Transactions*, 66(25):1–
293 12, 2015.
- 294 * This paper shows the importance of temperature gradients on fuel cell degradation.
- 295 [PB10] J.G. Pharoah and O.S. Burheim. On the temperature distribution in polymer electrolyte fuel cells. *Journal of Power Sources*,
296 195:5235–5245, 2010.
- 297 [RLDM08] J. Ramousse, O. Lottin, S. Didierjean, and D. Mailet. Estimation of the thermal conductivity of carbon felts used as PEMFC gas
298 diffusion layers. *Int. J. of Thermal Sci.*, 47:1–6, 2008.
- 299 [Roc87] A.L. Rockwood. Absolute half-cell entropy. *Physical Review Part A*, 36:1525–1526, 1987.
- 300 [ROHS95] Signe Kjelstrup Ratkje, Magnar Ottøy, Rune Halseid, and Monica Strømgaard. Thermoelectric power relevant for the solid-polymer-
301 electrolyte fuel cell. *Journal of membrane science*, 107(3):219–228, 1995.
- 302 [RRS02] P.J. Reucroft, D. Rivin, and N.S. Schneider. Thermodynamics of nafion-vapor interactions. I. Water vapor. *Polymer*, 43:5157–5161,
303 2002.
- 304 [SBD08] E. Sadeghi, M. Bahrami, and N. Djilali. Analytic determination of the effective thermal conductivity of PEM fuel cell gas diffusion
305 layers. *J. Power Sources*, 179:200–208, 2008.
- 306 [SDB10] E. Sadeghi, N. Djilali, and M. Bahrami. Effective thermal conductivity and thermal contact resistance of gas diffusion layers in
307 proton exchange membrane fuel cells. part 2: Hysteresis effect under cyclic compressive load. *J. Power Sources*, 195:8104–8109,
308 2010.
- 309 [SDB11] E. Sadeghi, N. Djilali, and M. Bahrami. A novel approach to determine the in-plane thermal conductivity of gas diffusion layers in
310 proton exchange membrane fuel cells. *J. Power Sources*, 196:3565–3571, 2011.
- 311 [SENVs04] N.P Siegel, M.W. Ellis, D.J. Nelson, and M.R. von Spakovsky. A two-dimensional model of a PEMFC with liquid water transport.
312 *Journal of Power Sources*, 128:173–184, 2004.

- 313 [SS85] S. Shibata and M.P. Sumino. The electrochemical peltier heat for the adsorption and desorption of hydrogen on a platinumized platinum
314 electrode in sulfuric acid solution. *J. Electroanal. Chem. Interfacial Electrochem.*, 193:135–143, 1985.
- 315 [SYG07] Yuyan Shao, Geping Yin, and Yunzhi Gao. Understanding and approaches for the durability issues of pt-based catalysts for PEM
316 fuel cell. *Journal of Power Sources*, 171(2):558–566, 2007.
- 317 [THBM08] A. Turhan, K. Heller, J. S. Brenizer, and M. M. Mench. Passive control of liquid water storage and distribution in a pefc through
318 flow-field design. *Journal of Power Sources*, 180:773 – 783, 2008.
- 319 [TKL11] P. Teertstra, G. Karimi, and X. Li. Measurement of in-plane effective thermal conductivity in PEM fuel cell diffusion media.
320 *Electrochimica Acta*, 56(3):1670–1675, 2011.
- 321 [TMD⁺13] A Thomas, G Maranzana, S Didierjean, J Dillet, and O Lottin. Measurements of electrode temperatures, heat and water fluxes in
322 PEMFCs: Conclusions about transfer mechanisms. *J. Electrochem. Soc.*, 160(2):F191–F204, 2013.
- 323 [TMD⁺14] A Thomas, G Maranzana, S Didierjean, J Dillet, and O Lottin. Thermal and water transfer in PEMFCs: Investigating the role of the
324 microporous layer. *Int. J. of Hydrogen Energy*, 39:2649–2658, 2014.
- 325 * This paper measures in situ heat fluxes in PEM fuel cells and as such is calorimetry. It also directly measures a
326 temperature difference caused by the presence of the MPL.
- 327 [US] US Department of Energy. Fuel cell technologies office information resources. [http://energy.gov/eere/fuelcells/fuel-cell-](http://energy.gov/eere/fuelcells/fuel-cell-technologies-office-information-resources)
328 [technologies-office-information-resources](http://energy.gov/eere/fuelcells/fuel-cell-technologies-office-information-resources). Accessed: 2016-05-25.
- 329 [VK04] P.J.S. Vie and S. Kjelstrup. Thermal conductivities from temperature profiles in the polymer electrolyte fuel cell. *Electrochimica*
330 *Acta*, 49:1069–1077, 2004.
- 331 [WG13] Y Wang and M. Gundevia. Measurement of thermal conductivity and heat pipe effect in hydrophilic and hydrophobic carbon papers.
332 *Int. J. Heat Mass Transf.*, 60:134–142, 2013.
- 333 [WN06] Adam Z Weber and John Newman. Coupled thermal and water management in polymer electrolyte fuel cells. *Journal of The*
334 *Electrochemical Society*, 153(12):A2205–A2214, 2006.
- 335 [XLCM14] G. Xu, J. M. LaManna, J.T. Clement, and M. M. Mench. Direct measurement of through-plane thermal conductivity of partially
336 saturated fuel cell diffusion media. *J. Power Sources*, 256:212–219, 2014.
- 337 [YANB12] J. Yableckia, A. A. Nabovati, and A. Bazylak. Modeling the effective thermal conductivity of an anisotropic gas diffusion layer in a
338 polymer electrolyte membrane fuel cell. *J. Electrochem. Soc.*, 159:B647–B653, 2012.
- 339 [ZKS⁺06] J. Zhang, D. Kramer, R. Shimoi, Y. Ono, E. Lehmann, A. Wokaun, K. Shinohara, and G. Scherer. In situ diagnostic of two-phase
340 flow phenomena in polymer electrolyte fuel cells by neutron imaging part b. material variations. *Electrochimica Acta*, 51:2715–2727,
341 2006.
- 342 [ZL13] N. Zamel and Xiangou Li. Effective transport properties for polymer electrolyte membrane fuel cells – with a focus on the gas
343 diffusion layer. *Progress in Energy and Combustion Sci.*, 39:146, 2013.
- 344 [ZLBW11] Nada Zamel, Xianguo Li, Jürgen Becker, and Andreas Wiegmann. Effect of liquid water on transport properties of the gas diffusion
345 layer of polymer electrolyte membrane fuel cells. *International Journal of Hydrogen Energy*, 36(9):5466–5478, 2011.
- 346 [ZLE⁺16] I.V. Zenyuk, A. Lamibrac, J. Eller, Y. Parkinson, D. F. Marone, F.N. Büchi, and Weber A.Z. Investigating evaporation in gas diffusion
347 layers for fuel cells with x-ray computed tomography. *Physical Chemistry C*, 120:28701–28711, 2016.
- 348 ** This article presents measurements of evaporation rates in fuel cell materials as well as modelling results covering
349 a good range of fuel cell operating conditions.
- 350 [ZLS⁺11a] N. Zamel, E. Litovsky, S. Shakhshir, X. Li, and J. Kleiman. Measurement of in-plane thermal conductivity of carbon paper diffusion
351 media in the temperature range of -20 °c to +120 °c. *Appl. Energy*, 88:3042–3050, 2011.
- 352 [ZLS⁺11b] N. Zamel, E. Litovsky, S. Shakhshir, X. Li, and J. Kleiman. Measurement of the through-plane thermal conductivity of carbon paper
353 diffusion media for the temperature range from -50 to +120 °c. *Int. J. Hydrogen Energy*, 36:12618–12625, 2011.
- 354 [ZW15] Iryna V Zenyuk and Adam Z Weber. Understanding liquid-water management in pefcs using x-ray computed tomography and
355 modeling. *ECS Transactions*, 69(17):1253–1265, 2015.